MISES Implementation
of Modified Abu-Ghannam/Shaw Transition Criterion
(Second Revision)

Mark Drela, MIT Aero-Astro

July 1998

1   Ill-posedness of the AGS criterion

The Abu-Ghannam/Shaw (AGS) transition-start criterion developed in reference [1] is defined in terms of the momentum-thickness Reynolds number R_θ, freestream turbulence level τ (in %), and the Thwaites parameter λ:

$$\text{AGS criterion:} \quad R_\theta \;=\; R_{\theta_S}(\lambda, \tau) \tag{1}$$

$$\text{where} \quad \lambda \;\equiv\; \frac{\theta^2}{\nu}\frac{du_e}{dx} \tag{2}$$

$$R_{\theta_S} \;=\; 163 \;+\; \exp\left[F(\lambda)\left(1 \;-\; \frac{\tau}{6.91} \right)\right] \tag{3}$$

$$F \;=\; \begin{cases} 6.91 \;+\; 12.75\lambda \;+\; 63.64\lambda^2 & \lambda < 0 \\ 6.91 \;+\; 2.48\lambda \;-\; 12.27\lambda^2 & \lambda > 0 \end{cases} \tag{4}$$

This was found to be ill-posed when incorporated into MISES. The cause is grounded in flow physics and not numerics, and this criterion would appear to be ill-posed when used in any flow solution method which fully resolves the viscous/inviscid interaction mechanism.

The ill-posedness arises from the influence of transition on the upstream boundary layer via the potential flow and the viscous displacement effect. When transition begins at x_{tr}, both δ^* and H first decrease rapidly from their laminar values. The transition region therefore looks like a sink to the potential flow. This effective sink accelerates the upstream potential flow $u_e(x)$ towards the transition onset point and drives λ more positive. This therefore simultaneously decreases R_θ and increases R_{θ_S}, as shown in Figure 1. Although this effect on u_e and surface pressure is quite small as far prediction of blade loading is concerned, it is usually strong enough locally so that R_θ and R_{θ_S} *diverge* towards the transition location. The result is that the AGS criterion (1) cannot hold at the transition onset point without also being triggered upstream — a direct contradiction. In practice, as the viscous displacement takes effect and R_θ and R_{θ_S} diverge, transition will jump far downstream in the next iteration of the code. With further iterations, it will propagate upstream, only to jump back downstream again and repeat the cycle. There is no stable overall solution. An intersection of R_θ and R_{θ_S} might be obtained if a coarse grid is used so that the displacement effect is "lost" inside one grid cell, but this is not guaranteed. Also, relying on inadequate resolution to obtain a solution is a dubious proposition!
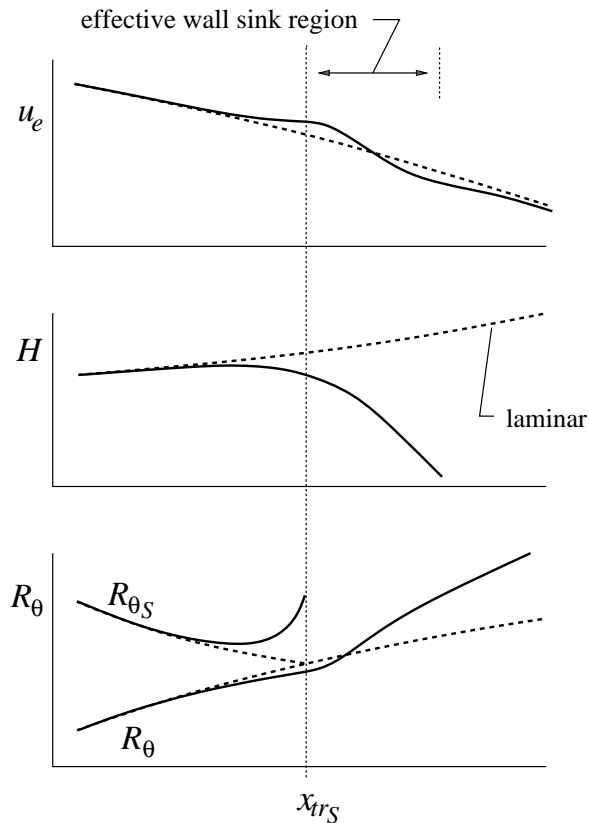
Figure 1: Behavior of boundary layer variables in the vicinity of transition.

2 Parameterization with H

The first step towards formulating a well-posed version of the original AGS criterion was to replace the dependence on λ with a dependence on H, so that equation (1) is now expressed as

$$R_\theta = R_{\theta_S}(H, \tau) \tag{5}$$

If Thwaites method is being used, λ and H are of course uniquely related, so in that case the change would be trivial. With the two-equation BL formulation used in MISES, however, they are not uniquely related, with H lagging λ somewhat. Using H instead of λ to parameterize boundary layer instability growth is theoretically more sound, since the pressure gradient does not have a direct bearing on the growth. As can be seen from the Orr-Sommerfeld equation, the direct effect comes from the mean profile shape $u(y)$ which is better described by H, and doesn't involve local dynamic equilibrium assumptions like the Thwaites' $H(\lambda)$ relation.

Using λ also has the fundamental problem in that it cannot be used in separating flows. In an actual flow with laminar separation, $\lambda \simeq -0.09$ is at its minimum at the separation point. Past the separation point it returns back to zero, increasing R_{θ_S}. At the same time, R_θ levels off. This can be seen from the appropriate form of the integral momentum

2

equation.

$$\frac{1}{R_\theta}\frac{dR_\theta}{dx} = \frac{1}{\theta}\frac{C_f}{2} - (H+1)\frac{1}{u_e}\frac{du_e}{dx} \tag{6}$$

Since both C_f and du_e/dx become nearly zero over the separated zone, dR_θ/dx becomes nearly zero as well. Hence, if equation (1) doesn't signal transition before laminar separation, it never will, no matter what the $R_{\theta_S}(\lambda)$ dependence is. This is at odds with common sense. With equation (5), the $R_{\theta_S}(H)$ dependence can at least be set up so that R_{θ_S} keeps decreasing as H increases past laminar separation, and hopefully will drop below R_θ. Of course, the AGS criterion was never meant to be applicable to separating flows, but in the interest of program robustness, strongly non-physical behavior is undesirable.

In any case, using H instead of λ improved the behavior somewhat, since in the two-equation BL method in MISES (and in finite-difference BL methods), H does not respond immediately to the increase in λ upstream of transition because of the inertial lags being represented. This reduces the divergence of R_θ and $R_{\theta_S}(H,\tau)$ towards transition. Nevertheless, in many cases these quantities still do not cross in a well-defined manner, especially in near-zero pressure gradients where the $R_{\theta_S}(H)$ sensitivity is the strongest, and R_{θ_S} is affected by the displacement mechanism the most.

3   Implementation via existing e^n formulation

The final approach taken was to modify the existing e^n envelope criterion in MISES to account for the presence of bypass transition. The present e^n criterion is

$$n(x_{\text{tr}}) = n_{\text{crit}}(\tau) \tag{7}$$

$$\text{where} \qquad n(x_{\text{tr}}) = \int_{x_o}^{x_{\text{tr}}} f(H, R_\theta)\,\frac{dx}{\theta} \tag{8}$$

$$n_{\text{crit}}(\tau) = -8.43 - 2.4\ln(\tau/100) \tag{9}$$

and the $n_{\text{crit}}(\tau)$ formula is Mack's correlation [2]. The integration for $n(x_{\text{tr}})$ is not performed explicitly, but rather the equivalent differential equation and initial condition are solved together with the inviscid flow and the other BL equations.

$$\theta\frac{dn}{dx} = f(H, R_\theta) \tag{10}$$

$$n(x_o) = 0 \tag{11}$$

It is possible to directly compare the AGS and e^n criteria for similar flows with constant H and λ, since for such flows the two versions of the AGS criterion (1) and (5) are equivalent. Figure 2 compares $R_{\theta_S}(\tau)$ from the AGS criterion and $R_\theta(x_{\text{tr}}(\tau))$ implied by the e^n criterion. The corresponding curves cross near the Blasius flow value $H = 2.6$, so that for adverse pressure gradients, the e^n criterion will likely be triggered first, while for favorable pressure gradients the AGS criterion will likely be triggered first. With most adverse

pressure gradient flows found on airfoils, $H(x)$ is not constant but increases downstream towards separation and/or transition. In this case, the R_θ at transition predicted by e^n for $H > 2.6$ will be larger than the curves in Figure 2, and will be closer to the AGS criterion. The conclusion here is that in the AGS experiments the adverse pressure gradient cases quite likely involved significant TS-wave growth, and transition was most likely not the result of direct bypass transition. The AGS criterion therefore represents bypass transition in favorable pressure gradients, but mostly TS-wave transition in adverse pressure gradients. The relatively recent experiments of Westin et al [3] indicate that in fact TS waves play a role in the transition process even with large freestream turbulence levels, although they are difficult to distinguish among the externally-imposed "noise". They also argue that the term "bypass transition" is difficult to define, since both linear (TS-wave) and non-linear mechanisms are always at work.
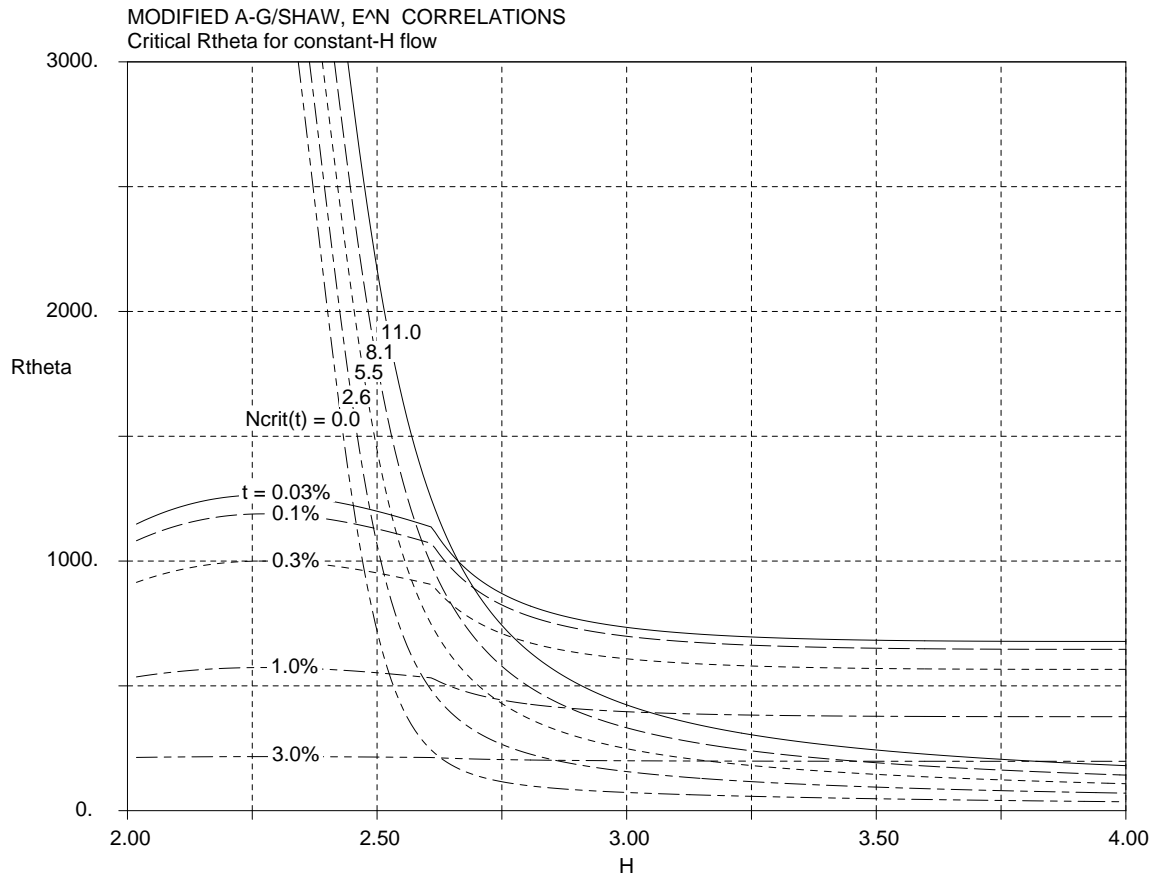

Figure 2: Critical R_θ versus shape parameter H for similar flows. Comparison of e^n method and AGS method predictions.

All these results indicate that the TS-wave and bypass transition mechanisms are not as distinct as was once believed — in most flows both mechanisms participate to varying degrees. This suggested that an appropriate implementation of the AGS criterion might be via a modification of the existing e^n method, preferably in a manner which eliminates the

inherent ill-posedness of the standard AGS criterion. The first step is to modify Mack's relation to admit arbitrarily large turbulence levels. The standard relation (9) produces negative n_{crit} values for $\tau > 2.98\%$, which makes no physical sense. This is not too surprising, since Mack's relation was developed for low turbulence flows. The modified definition is

$$\tau' = 2.7 \tanh(\tau/2.7) \tag{12}$$

$$\tilde{n}_{crit}(\tau) = -8.43 - 2.4 \ln\left(\frac{\tau'}{100}\right) \tag{13}$$

which now results in $\tilde{n}_{crit}$ asymptoting to near-zero for large values of τ, and becomes equivalent to Mack's original relation for small values of τ. The inverse form is also useful to note.

$$\tau' = 100 \exp\left(-\frac{8.43 + \tilde{n}_{crit}}{2.4}\right)$$

$$\tau(\tilde{n}_{crit}) = \frac{2.7}{2} \ln\left(\frac{1 + \tau'/2.7}{1 - \tau'/2.7}\right)$$

The second step is the replacement of the original AGS $R_{\theta_S}(\lambda, \tau)$ definition (3) with the alternative form

$$R_{\theta_S}(H, \tilde{n}_{crit}) = 155 + 89.0 \left[0.25 \tanh\left(\frac{10}{H-1} - 5.5\right) + 1\right] (\tilde{n}_{crit})^{1.25} \tag{14}$$

which in addition to relying on H in lieu of λ, also uses $\tilde{n}_{crit}(\tau)$ in lieu of τ itself. Because $\tilde{n}_{crit}$ and τ are defined to be uniquely related, the latter change is trivial, and is done for convenience.

Assuming Thwaites' $H(\lambda)$ relation, which for Falkner-Skan flows is closely approximated by

$$\lambda(H) = \frac{0.058(H-4)^2}{H-1} - 0.068 \tag{15}$$

and also assuming the modified Mack's $\tilde{n}_{crit}(\tau)$ correlation, equation (14) returns substantially the same R_{θ_S} values as the original AGS formula (1), particularly for favorable pressure gradients and large τ values. Both forms fall well within the scatter of the data presented by Abu-Ghannam–Shaw [1] in their Figure 6. The new form (14) is well-defined for all values of H, which helps to produce a more robust code. For τ below 0.5%, the two forms begin to depart significantly, with the AGS $R_{\theta_S}(\lambda, \tau)$ approaching a constant upper limit, while the new form $R_{\theta_S}(H, \tilde{n}_{crit})$ grows without bound (although only logarithmically). The latter behavior arises from the logarithmic dependence in equation (13), and is theoretically correct for the TS wave transition mechanism.

The actual implementation of the new R_{θ_S} criterion is completed by redefining the overall growth rate in the amplification factor $n(x)$ as

$$\theta \frac{dn}{dx} = f(H, R_\theta) + g(H, R_\theta) \tag{16}$$

5

where f is the original Orr-Sommerfeld-based TS wave growth rate, and g is a new contribution defined as:

$$g(H, R_\theta) = \begin{cases} 0 & r < 0 \\ A\,(3r^2 - 2r^3) & 0 < r < 1 \\ A & r > 1 \end{cases} \tag{17}$$

$$r = \frac{1}{B}\left(\frac{R_\theta}{R_{\theta_S}} - 1\right) + \frac{1}{2} \tag{18}$$

$$A = 0.10 \tag{19}$$

$$B = 0.30 \tag{20}$$

Essentially, a very large fictitious growth rate $g(H, R_\theta) = A$ is introduced as R_θ approaches R_{θ_S} (for a Blasius flow, $f(H, R_\theta) \simeq 0.002$, or about 50 times smaller). This rapid additional growth rate is brought in somewhat gradually via the cubic ramp function to alleviate any potential numerical problems. Once this term activates, transition onset will occur roughly within a streamwise distance of about $\theta \times \tilde{n}_{\mathrm{crit}}/A$, or about 1–10 boundary layer thicknesses, depending on $\tilde{n}_{\mathrm{crit}}$.

In practice, the details of the cubic ramp function have little effect on the transition location relative to the blade chord. The cubic ramp serves to innoculate the method from the sudden divergence of R_{θ_S} and R_θ as transition is approached (Figure 1). As long as R_{θ_S} and R_θ do not diverge by more than the ramp width $\sim R_{\theta_S} B/2$, then dn/dx will remain positive enough to still trigger transition shortly downstream. The method can be made better-behaved by increasing the ramp width parameter B, but it will then depart further from the local character of the AGS criterion (which may or may not be a drawback).

In adverse pressure gradients and/or very small τ (large $\tilde{n}_{\mathrm{crit}}$) levels, the g function does not activate before the f function causes a critical growth in $n(x)$, while in favorable pressure gradients and/or large τ levels, the g function dominates. This mimics the dominance of the bypass transition mechanism in the former situation, and the TS-wave mechanism in the latter situation.

Figure 3 shows the BL variable distributions for a case with a slow initial growth in $n(x)$ due to the $f(H, R_\theta)$ TS-wave term, with a very rapid growth then being triggered by the $g(H, R_\theta)$ bypass transition term as R_θ approaches R_{θ_S}. Note the slight acceleration in u_e and a corresponding decrease in H as transition is approached, and the resulting sudden divergence between R_θ and $R_{\theta_S}(H, \tilde{n}_{\mathrm{crit}})$ just before transition onset.

The original AGS $R_{\theta_S}(\lambda, \tau)$ is also shown as a dotted line, although it does not participate in the calculation. Its erratic behavior is partially due to the dependence of λ on the finite difference $\Delta u_e/\Delta x$ which is obviously much more sensitive to numerical noise than just H. The slope discontinuity at $x = 0.25$ is due the slope discontinuity of the $F(\lambda)$ function at $\lambda = 0$.

It is unlikely that a well-behaved transition criterion based on λ could have been derived. A fine streamwise grid resolution was used to demonstrate the behavior, but the resultant transition location is essentially unchanged with more practical resolution.

4   Transition intermittency

The overall AGS formulation in reference [1] incorporates an intermittency factor γ based on R_θ development over the transition region.

$$\gamma = 1 - \exp(-5\eta^3) \tag{21}$$

$$\eta = \frac{R_\theta - R_{\theta_S}}{R_{\theta_E} - R_{\theta_S}} \tag{22}$$

The Reynolds number R_{θ_E} at the end of the transition zone is in turn correlated to various parameters at the transition-onset point and local flow properties. The correlations were obtained from a range of flow situations in adverse and favorable pressure gradients. Unfortunately, such an approach is hopelessly inadequate if any flow separation occurs. Since R_θ no longer increases past laminar separation, η as defined by equation (22) levels off, and the intermittency γ ceases to increase! This result is clearly at odds with separation bubble data (see Liebeck [4], for example) which clearly shows that turbulence intensity reaches its full levels almost instantanously — within a few boundary layer thicknesses at most. Clearly, any reliable intermittency formulation which can tolerate separated flows cannot be tied to the downstream R_θ development.

The current MISES BL formulation incorporates a lag equation which governs the downstream evolution of the Reynolds stress coefficient $C_\tau = (-\overline{u'v'}/u_e^2)_{\max}$:

$$\frac{\delta}{C_\tau}\frac{dC_\tau}{dx} = K_C\left(C_{\tau_{EQ}}^{1/2} - C_\tau^{1/2}\right) + \dots \tag{23}$$

where δ is the BL thickness and $K_C = 5.6$ is the lag constant. The actual C_τ chases the local equilibrium value $C_{\tau_{EQ}}(H)$, which is derived from the $G - \beta$ turbulent equilibrium locus (see Green et al [5], for example). The initial value of C_τ at the transition-onset point is currently correlated with the shape parameter at that point:

$$C_\tau(x_{\mathrm{tr}}) = C_{\tau_{EQ}} \times 3.24 \exp\left(\frac{-6.6}{H-1}\right) \tag{24}$$

The exponential scaling factor has been developed from the extensive high-quality low Reynolds number separation bubble data of McGhee et al [6]. The basis of the correlation is the measured sharp adverse pressure gradient in the reattachment region of a separation bubble, which is controlled almost entirely by $C_\tau(x_{\mathrm{tr}})$. The values resulting from equation (24) are:

$$
\begin{aligned}
C_\tau(x_{\mathrm{tr}}) &= C_{\tau_{EQ}} \times 0.02 & ; \quad H = 2.3 \\
&= C_{\tau_{EQ}} \times 0.05 & ; \quad H = 2.6 \\
&= C_{\tau_{EQ}} \times 0.36 & ; \quad H = 4.0 \\
&= C_{\tau_{EQ}} \times 1.26 & ; \quad H = 8.0 \\
&= C_{\tau_{EQ}} \times 3.24 & ; \quad H = \infty
\end{aligned}
$$

Note that for favorable pressure gradients ($H < 2.6$), the initial C_τ is quite small, and takes some distance to approach $C_{\tau_{EQ}}$, while for a separation bubble, C_τ begins at or even above

its equilibrium value, reflecting the almost instantanous transition observed in separation bubbles.

For favorable pressure gradients, the gradual rise in C_τ predicted by the lag equation (23) qualitatively mimics the transition process, in that the Reynolds stresses and the skin friction require a finite downstream distance to reach their full level. However, this distance is predicted to be several times shorter than what is observed in typical flat-plate flows. Figure 4 shows computed results for a flat plate compared with data from Abu-Ghannam and Shaw [1]. There is some question as to the accuracy of the data in the laminar region, since the measured $H = 2.85$ there is far too high. In any case, the transition onset location is predicted quite well, but the rise in C_τ, which drives the rise in C_f and decrease in H is several times too fast. The result is that θ and hence R_θ is predicted to grow too fast until transition is complete.

Obviously, the lag equation does not simulate the turbulent spot formation process and intermittency in general. Reducing the rate constant in equation (23) to $K_C = 1.9$, or about 1/3 its current value, achieves the desired effect, but this also totally corrupts the ability of the code to accurately predict turbulent separation, and hence is unacceptable. There is no simple way to remedy this, short of introducing another rate equation modeling the turbulent spot formation and merging rate. In summary, there is another rate scale in the flow physics which must be represented by another differential equation. Non-local correlations such as the AGS intermittency function (21) achieve this by assuming that this rate is commensurate with growth rate of the momentum thickness Reynolds number. If the flow physics of the two processes are distinct, as they appear to be, this assumption can by valid only for a sufficiently narrow range of flows (i.e. Blasius-like flows). Not surprisingly, this approach fails seriously in the presence of separation.

Adding an additional rate equation to MISES to model the spot-formation process is not being contemplated at the moment. It is not appropriate for flows with laminar separation, since here transition is almost instantaneous and there is no gradual spot formation and merging process. Extensive experience with the isolated-airfoil version of MISES indicates that present formulation is quite reliable for cases with separation bubbles. For transition in neutral or favorable pressure gradients, MISES in its present form will simply predict that the skin friction immediately past transition onset is somewhat too high, and will predict slightly higher losses. As long as this behavior is recognized, the code remains a useful predictive tool.

5   Edge velocity change corrections

The standard e^n and AGS methods do not address the issue of a proper definition of the turbulence level τ and corresponding n_{crit} when the edge velocity u_e changes significantly over the streamwise extent of a boundary layer. This is certainly important in turbine cascades, where u_e can increase an order of magnitude from inlet to outlet. Resolving this issue requires examining the underlying assumptions inherent in the present transition

prediction methods, and including any u_e variations accordingly.

Linear stability theory describes the evolution of the *dimensional* velocity fluctuations u' inside the boundary layer. A key simplifying assumption of the present e^n envelope method is that the growth of u', which represents the amplitude of the most-amplified wave, can be approximated by the form

$$\frac{d \ln u'}{dx} = \frac{1}{\theta} f(H, R_\theta) \tag{25}$$

which assumes that θ and H suffice to fully characterize the mean profile via the dimensionless function f. This assumption is correct for the one-parameter Falkner-Skan profile family, and appears to be reasonably sound for non-similar flows.

This exponential growth of u' arises from a small background "noise" level u'_o which is assumed to depend nonlinearly on the ambient turbulence level outside the boundary layer.

$$u'_o = u_{\text{ref}} (K\tau)^b \tag{26}$$

Here, K and b are empirical constants representing the receptivity of the boundary layer to external turbulence, and u_{ref} is simply the reference velocity used to define τ. In airfoils the reference velocity u_{ref} is typically chosen to be the freestream velocity, and in cascades it is typically the inlet velocity. The choice is merely a matter of convention, and is not important here.

The assumption that K and b are constant for all locations along the boundary layer is perhaps questionable, but there is little more that can be done in the relatively simple present treatment. Equation (26) also assumes that the turbulence level persists at the fixed level τu_{ref} along the inviscid streamlines. This is certainly appropriate, since turbulent kinetic energy is not affected by mean-flow acceleration or deceleration.

It is commonly accepted that nonlinear breakdown to transition is initiated when the ratio u'/u_e reaches some small threshold value T.

$$\left.\frac{u'}{u_e}\right|_{x_{\text{tr}}} = T \tag{27}$$

Rapid nonlinear breakdown will then follow provided R_θ is large enough to support turbulence. A representative threshold is $T \simeq 0.01$, although this does not have to be chosen explicitly since only amplification ratios will be considered.

It is convenient at this point to quantify u' in terms of a modified amplification factor $\bar{n}$ which is referenced to the local u_e rather than the fixed u_{ref} assumed by the standard e^n methods.

$$\bar{n} \equiv \ln \frac{u'}{u_e} - \ln \frac{u'_o}{u_{\text{ref}}} = \ln \frac{u'}{u_e} - b \ln(K\tau) \tag{28}$$

The constant $K\tau$ bias term is included for convenience, so that $\bar{n} = 0$ at the reference condition before any growth occurs. With the definition

$$\bar{n}_{\text{crit}} = b \ln \frac{T}{K\tau} \tag{29}$$

9

the transition criterion (27) retains the standard form (7).

$$\bar{n}(x_{\text{tr}}) \;=\; \bar{n}_{\text{crit}} \tag{30}$$

Also, the u' rate equation (25) and its initial condition (26) reduce to the amplification relations (16, 11) if we also include the $g(H, R_\theta)$ bypass term. The key distinction is that additional terms involving u_e now appear.

$$\frac{d\bar{n}}{dx} + \frac{d\ln u_e}{dx} \;=\; \frac{1}{\theta}\left[f(H, R_\theta) + g(H, R_\theta)\right] \tag{31}$$

$$\bar{n}(x_o) \;=\; \ln\frac{u_{\text{ref}}}{u_e} \tag{32}$$

The initial condition (11) cannot be imposed if x_o is chosen to be the stagnation point, since here $u_e = 0$ and $\bar{n} = \infty$. However, the results of the method are unchanged if x_o is chosen to lie anywhere after the stagnation point but before f or g become nonzero. Selecting the first discrete location after the stagnation point is most convenient and is perfectly adequate. Note that unlike in the unmodified e^n method, $\bar{n}$ no longer necessarily starts at zero at x_o. Also, if $u_e(x)$ varies, then $\bar{n}(x)$ will also vary even before genuine amplification occurs via f or g.

Requiring consistency of the $\bar{n}$ definition (29) and Mack's correlation (9) results in the following values of the modeling constants.

$$b \;=\; 2.4$$
$$K \;=\; (T/100)\,\exp(8.43/b) \;=\; 0.33\,T$$

These values are given out of curiosity more than anything else, since they do not appear explicitly in the final form of the transition prediction method as embodied in equations (30, 31, 32).

References

[1] B.J. Abu-Ghannam and R. Shaw. Natural transition of boundary layers — The effects of turbulence, pressure gradient, and flow history. *Journal of Mechanical Engineering Science*, 22(5):213–228, 1980.

[2] L.M. Mack. Transition prediction and linear stability theory. In *AGARD-CP-224*, pages 1.1–1.22, 1977.

[3] K.J.A. Westin, A.V. Boiko, B.G.B. Klingmann, V.V. Kozlov, and P.H. Alfredsson. Experiments in a boundary layer subjected to free stream turbulence. Parts 1,2. *Journal of Fluid Mechanics*, 281(12):193–246, 1994.

[4] R.H. Liebeck. Laminar separation bubbles and airfoil design at low Reynolds numbers. AIAA-92-2735-CP, June 1992.

[5] J.E. Green, D.J. Weeks, and J.W.F. Brooman. Prediction of turbulent boundary layers and wakes in compressible flow by a lag-entrainment method. R & M Report 3791, Aeronautical Research Council, HMSO, London, 1977.

[6] R.J. McGhee, B.S. Walker, and B.F. Millard. Experimental results for the Eppler 387 airfoils at low Reynolds numbers in the Langley Low-Turbulence Pressure Tunnel. Technical Memorandum 4062, NASA, Oct 1988.
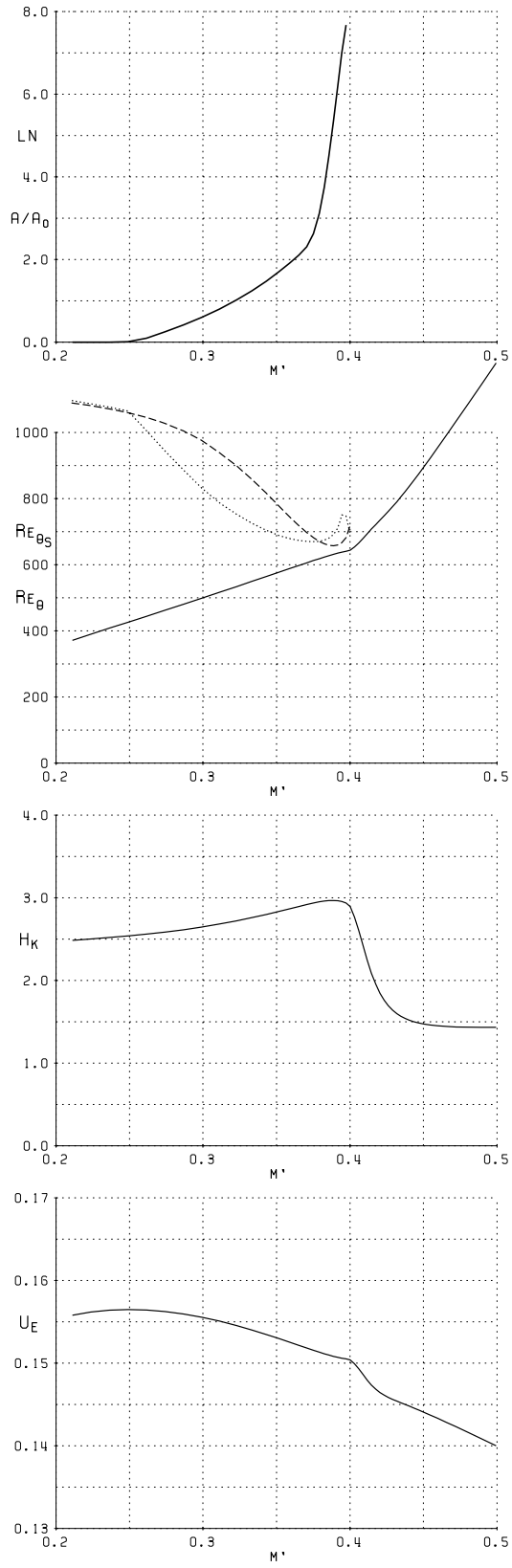
Figure 3: Boundary layer variable behavior in the vicinity of transition onset at $x_{\mathrm{tr}} = 0.40$, showing divergence of R_θ (solid line) and R_{θ_S} (dashed line). Original AGS $R_{\theta_S}(\lambda, \tau)$ is also shown as a dotted line.
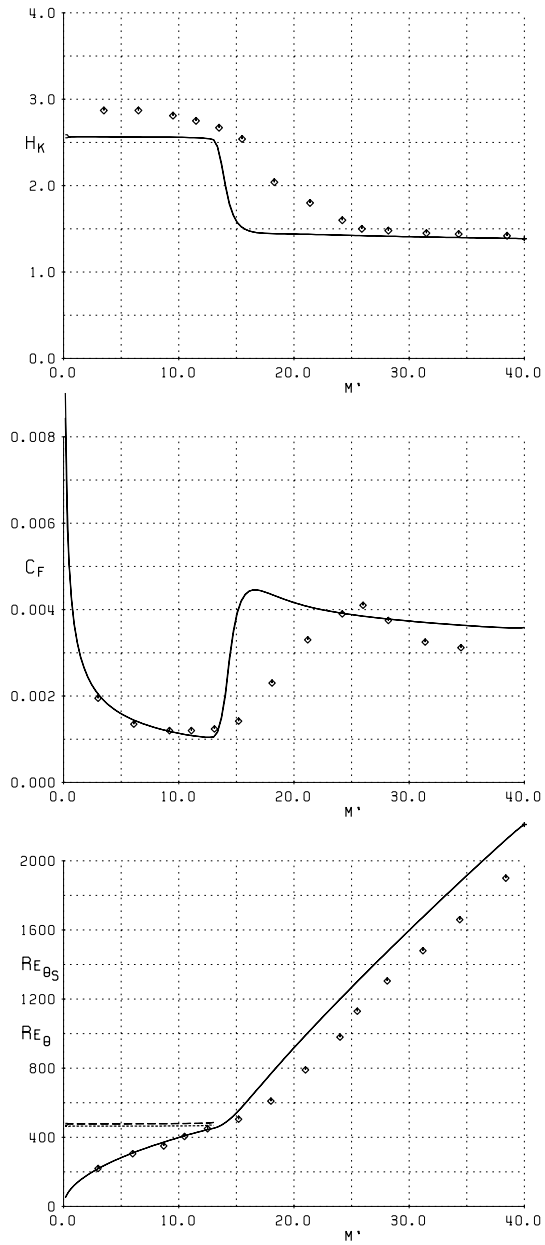
Figure 4: Predicted boundary layer quantities over a flat plate compared with experimental data. Zero pressure gradient, $\tau = 1.25\%$. Experimental $x_{\mathrm{tr}} = 13.0$